On the Truncation of Long-Range Electrostatic Interactions in DNA

Jan Norberg and Lennart Nilsson
Center for Structural Biochemistry, Department of Bioscience at Novum, Karolinska Institutet, S-141 57 Huddinge, Sweden

ABSTRACT Long-range interactions are known to play an important role in highly polar biomolecules like DNA. In molecular dynamics simulations of nucleic acids and proteins, an accurate treatment of the long-range interactions are crucial for achieving stable nanosecond trajectories. In this report, we evaluate the structural and dynamic effects on a highly charged oligonucleotide in aqueous solution from different long-range truncation methods. Two group-based truncation methods, one with a switching function and one with a force-switching function were found to fail to give accurate stable trajectories close to the crystal structure. For these group-based truncation methods, large root mean square (rms) deviations from the initial structure were obtained and severe distortions of the oligonucleotide were observed. Another group-based truncation scheme, which used an abrupt truncation at 8.0 Å or at 12.0 Å was also investigated. For the short cutoff distance, the conformations deviated far away from the initial structure and were significantly distorted. However, for the longer cutoff, where all necessary electrostatic interactions were included, the trajectory was quite stable. For the particle mesh Ewald (PME) truncation method, a stable DNA simulation with a heavy atom rms deviation of 1.5 Å was obtained. The atom-based truncation methods also resulted in stable trajectories, according to the rms deviation from the initial B-DNA structure, of between 1.5 and 1.7 Å for the heavy atoms. In these stable simulations, the heavy atom rms deviations were ~0.6–1.0 Å lower for the bases than for the backbone. An increase of the cutoff radius from 8 to 12 Å decreased the rms deviation by ~0.2 Å for the atom-based truncation method with a force-shifting function, but increased the computational time by a factor of 2. Increasing the cutoff from 12 to 18 Å for the atom-based truncation method with a force-shifting function requires 2–3 times more computational time, but did not significantly change the rms deviation. Similar rms deviations from the initial structure were found for the atom-based method with a force-shifting function and for the PME method. The computational cost was longer for the PME method with a cutoff of 12.0 Å for the direct space nonbonded calculations than for the atom-based truncation method with a force-shifting function and a cutoff of 12.0 Å. If a nonperiodic boundary, e.g., a spherical boundary, was used, a considerable speedup could be achieved. From the rms fluctuations, the terminal nucleotides and especially the cytidines were found to be more flexible than the nonterminal nucleotides. The B-DNA form of the oligonucleotide was maintained throughout the simulations and is judged to depend on the parameters of the energy function and not on the truncation method used to handle the long-range electrostatic interactions. To perform accurate and stable simulations of highly charged biological macromolecules, we recommend that the atom-based force-shift method or the PME method should be used for the long-range electrostatics interactions.

INTRODUCTION

Nucleic acids structures are highly charged molecules (Saenger, 1988) for which an accurate treatment of the long-range interactions is very important. Nonbonded interactions between atoms or groups are usually truncated at a specific cutoff distance to reduce the number of interactions and thereby the required computational time for the molecular dynamics (MD) simulation (McCammon and Harvey, 1987). The importance of long-range interactions in biomolecular systems has been reviewed (Berendsen, 1993; Harvey, 1989; Smith and van Gunsteren, 1993). Here, we will describe a number of studies that have focused on the advantages or disadvantages of different methods for treating the long-range electrostatic interactions and that make up the basis for the present investigation.

Received for publication 10 March 2000 and in final form 12 June 2000.
Address reprint requests to Jan Norberg, Center for Structural Biochemistry, Department of Bioscience at Novum, Karolinska Institutet, S-141 57 Huddinge, Sweden. Tel.: +46-8-608-9264; Fax: +46-8-608-9290; E-mail: Jan.Norberg@biosci.ki.se.

0006-3495/00/09/1537/17 $2.00

A solvated 17-residue peptide has been used (Schreiber and Steinhauser, 1992a,b,c) to analyze the effects from different cutoff radii using the charge-group approach for the Coulombic interactions compared to the Ewald technique (Ewald, 1921). The helix stability was preserved by using the Ewald technique, whereas, for the charge-group approach, the cutoff of 14.0 Å was judged to be too short from a 90-ps simulation (Schreiber and Steinhauser, 1992a).

The protein *Streptomyces griseus* protease A was simulated (Kitson et al., 1993) in its crystal environment using the twin-range method (Berendsen et al., 1986) with a long cutoff of 25.0 Å. In the 187-ps simulation, the root mean square deviation from the experimental structure was ~0.6–0.8 Å. In another study (Saito, 1994), human lysozyme was simulated in aqueous solution for 400 ps in two ways using a residue-based cutoff of 10.0 Å and the particle–particle and particle–cell method (Saito, 1992). The study clearly showed larger root mean square (rms) deviation values for the residue-based cutoff method.

A comparison between the Ewald and the switching function techniques was performed for a zwitterionic pentapeptide in aqueous solution (Smith and Pettitt, 1991). The flexibility of the peptide was reduced when using the

switching function, which also distorted the long-range electrostatic potential at the used cutoff of 9–10 Å. Further, the efficiency of the Ewald technique was improved by separating the real space sum into a short-range and a long-range part and using a multiple time step algorithm (Smith and Pettitt, 1995). The method was found to be slightly more expensive than using a conventional cutoff method. It was also argued in the study that potential "enhanced periodicity" effects could be eliminated. In another study, the anisotropic nature of the Ewald potential was analyzed (Smith and Pettitt, 1996). The rotational Ewald artífacts resulting from artificial periodicity were observed to be negligible above a certain temperature. It was further argued that the Ewald artifacts are totally negligible for solvents with high relative permittivity (Smith and Pettitt, 1996).

A particle mesh Ewald (PME) method based on interpolation of the reciprocal space Ewald sums has been developed (Darden et al., 1993). The method is of order $N \cdot \log(N)$ and further uses fast Fourier transformations to evaluate the convolutions of the energy and force. A 40% overhead compared to truncation list-based methods was obtained for macromolecular systems. This method has been extended using B-spline interpolation of the reciprocal space structure factors (Essmann et al., 1995). The protein HIV-1 protease was simulated for 300 ps in its crystal environment using a residue-based nonbond list with a cutoff of 9.0 Å and with a twin-range 9/18 Å cutoff (York et al., 1993). The same protein crystal was also simulated using the PME method and compared to the cutoff simulations. In the study the Ewald, crystal simulation was found to agree best with the crystallographic data (York et al., 1993).

In ionic and polar fluids the effect on the electrostatic interactions was investigated for six Coulombic potential truncation schemes (Brooks et al., 1985). The truncation scheme that uses a shift to make the force continuous and zero at the cutoff, and also includes a term that shifts the potential to zero at the cutoff, showed the smallest effect on the site–site distribution functions for water. This scheme also gave the smallest perturbation in the shape of the potential at distances shorter than the cutoff (Brooks et al., 1985).

An extensive study (Loncharich and Brooks, 1989) focused on carboxymyoglobin and analyzed six methods of truncating the long-range interactions in seventy 150-ps gas-phase MD simulations. Large rms deviations were observed using a shifted potential and cutoffs shorter than 14 Å. The switching function was found to perform badly using a short range to switch off the potential. It was also claimed that an atom-based switching function should not be used with a constant dielectric. For short cutoffs, the group–group distance-based truncation method showed larger rms deviations than for the atom–atom truncation method, though, at longer cutoffs, the difference was less (Loncharich and Brooks, 1989).

In a study of bovine pancreatic trypsin inhibitor, the protein dynamics was evaluated for implicit and explicit solvent models. The study found that good solvation properties could be obtained using a thin shell of water with either a distance-dependent dielectric or a constant dielectric model (Guenot and Kollman, 1992). A following study (Guenot and Kollman, 1993) evaluated the effects of truncating long-range interactions in simulations on the bovine pancreatic trypsin inhibitor protein, which was solvated by a 4-Å water shell. The constant dielectric and distance-dependent dielectric models with or without a switching function and a cutoff were examined. A linear distance-dependent dielectric model was shown to give better results than a constant dielectric model with a small hydration shell (Guenot and Kollman, 1993).

An atom-based force-switching method and a group-based method, which first shifts the energy interaction between two groups and then uses a switching function, were developed and compared to other truncation methods (Steinbach and Brooks, 1994). In the study, a generalized atom-based force-shifting method was presented. Thirty-five 150-ps simulations of carboxymyoglobin solvated in a layer of water were carried out, and poor results were found for the atom-based potential switching and the group-based potential switching methods. The atom-based force-shifting and force-switching methods, together with the switched group-shift method performed best. It was further argued that applying a cutoff of 12.0 Å or longer is more important than choosing a specific truncation method (Steinbach and Brooks, 1994).

The effect from long-range interactions on transport and interfacial properties of water has been examined for both spherical truncation and Ewald summation methods (Feller et al., 1996). The atom-based force truncation methods caused increased ordering of the fluid that changed the surface and transport properties. Most properties were found to agree best with experiment when the PME method was applied. An interesting result is that the relative force error for periodic systems was observed to be significantly lower in the PME calculations than in the spherical cutoff methods (Feller et al., 1996). Another MD investigation (Prevost et al., 1990) of pure water found similar results for the force-shift truncation method and the Ewald summation method and poor results for the shifting function.

The PME method has been applied to two double-stranded RNA dinucleotides in their crystal environment and the obtained rms deviations were ~0.4 Å for the heavy atoms (Lee et al., 1995). In the same study, one of the RNA dinucleotides was simulated in aqueous solution and then the heavy atoms rms deviation was found to be 1.02 Å. The PME method has also been applied in the 5- and 12-ns solution simulations of the $d(CCAACGTTGG)_2$ decamer

(Bevan et al., 2000). In the analysis, the rms deviations from the crystal structure were found to be 4.22 Å.

The dodecamer d(CGCGAATTCGCG)$_2$ has been simulated for 500 ps using the PME method in aqueous solution (Miaskiewics et al., 1996). An rms deviation of 2.5 Å for the heavy atoms was obtained from the minimized B-DNA starting structure. This dodecamer has also been simulated in the crystal unit cell using the PME method and then the rms deviation from the crystal structure was 1.16 Å for the heavy atoms (York et al., 1995). An aqueous solution MD simulation of the dodecamer has been conducted using the Ewald method for 3.5 ns (Yang and Pettitt, 1996). A stable trajectory was found with an rms deviation from the B-DNA structure estimated to ~5 Å. This dodecamer has also been simulated for 5 ns using the PME method (Young et al., 1997). The study analyzed the solvent dynamics and observed an rms deviation of 2.88 Å from the crystal structure. In another solution MD study of the d(CGCGAATTCGCG)$_2$ dodecamer, the potential was shifted to zero at a 12.0 Å cutoff (MacKerell, 1997). The study showed stable trajectories closer to the A-DNA form than to the B-DNA form and the rms deviations varied approximately from 4 to 5.5 Å from the starting structure. Stable trajectories of the B-DNA dodecamer d(CGCGCGCGCGCG)$_2$ have also been obtained for different pressures using an atom-based approach and a force-shifting function (Norberg and Nilsson, 1996a). The study also found that the corresponding A-RNA form of the dodecamer gave even more stable trajectories with rms deviations of 1.25 Å from the initial structure.

A comparison between the PME method and two charge group-based truncation cutoff methods was performed for the d(CCAACGTTGG)$_2$ decamer in aqueous solution (Cheatham et al., 1995). Significant structural distortions of the decamer with rms deviations <6 Å from the crystal structure were found for the charge group-based truncation cutoff methods. In contrast, for the PME method, the rms deviation was 3.2 Å from the crystal structure. The same solvated decamer was also simulated starting from its A-DNA and B-DNA forms using the PME method in the production phase (Cheatham and Kollman, 1996). The corresponding crystal structure is more in the B-DNA form, 1.71-Å rms deviation, than in the A-DNA form, 5.96-Å rms deviation. In the study (Cheatham and Kollman, 1996), the rms deviations from the A-DNA, B-DNA, and the crystal structure were 3.4–4.1 Å, 2.9–3.3 Å, and 3.1–3.6 Å, respectively.

In an investigation of the d(CGCGAAAAAACG)$_2$ dodecamer using the PME method, the effect of different box sizes was analyzed (Norberto de Souza and Ornstein, 1997a). The study used different box sizes and found all-atom rms deviations of 4.4–4.7 Å, 3.3–3.6 Å, and 2.9–3.3 Å from the A-DNA, B-DNA, and crystal structure, respectively. MD simulations (Norberto de Souza and Ornstein, 1997b) have also been carried out for the B-DNA dodecamer d(GCTATAAAAGGG)$_2$ in aqueous solution using the PME method. In the investigation, rms deviations were obtained to vary from 4.11 to 4.97 Å from the initial B-DNA structure (Norberto de Souza and Ornstein, 1997b). The same research group also investigated a protein–protein dimer using the PME method and a residue-based cutoff method with a cutoff radius of 10 Å (Norberto de Souza and Ornstein, 1999). They found all heavy-atom rms deviations of 1.3 and 4.7 Å for the PME and cutoff method, respectively, and concluded that the PME method is far superior over the cutoff method, which can be catastrophic for large protein complexes.

The d(CGCGAATTCGCG)$_2$ duplex has been simulated in aqueous solution starting from the A-DNA and the B-DNA form using the PME method to truncate the long-range interactions (Cieplak et al., 1997). In the report, it is pointed out that the PME method is necessary to simulate accurate behavior of oligonucleotides in crystals and aqueous solution. From the simulations, rms deviations of 4.4–4.7 Å, 3.1–3.3 Å, and 2.7–3.1 Å from the A-DNA, B-DNA, and crystal structure, respectively, were obtained (Cieplak et al., 1997). These rms deviation data are in close agreement with what has been found for a dodecamer elsewhere (Norberto de Souza and Ornstein, 1997a). Seven DNA dodecamers have been simulated (Pastor et al., 1997) in water using both spherical truncation cutoffs and the PME method. The study found rms deviations between 3.9 and 4.3 Å from the B-DNA form.

A DNA triple helix was simulated in water for 1.3 ns using the Ewald method, and the determined rms deviation was 1.89 Å from the initial structure (Weerasinghe et al., 1995). Another solution MD study (Shields et al., 1997) of a triplex has been performed starting from A-DNA and B-DNA conformations. The PME method was applied in the study and the resulting rms deviations were 2.2 and 1.4 Å from the A-DNA and B-DNA form, respectively. In another study, the PME method was used to investigate the dynamics of the crystal structure of yeast tRNA^{Asp} and the tertiary interactions were maintained throughout the simulation (Auffinger and Westhof, 1998). This was concluded to be due to the accurate treatment of the long-range electrostatic interactions.

Solution MD simulations (Duan et al., 1996) were performed of the DNA-*Eco*RI and DNA-EcoRV complexes using the PME method. In the study, the trajectories were found to be very stable, and this was claimed to be due to the PME method. This research group also published a study of the d(CGCGAATTCGCG)$_2$ dodecamer in aqueous solution using the PME method (Duan et al., 1997). The kinked starting structure transferred into a B-DNA structure during the 1-ns simulation. At the end of the trajectory, rms deviations of 3.53 Å from the B-form DNA and 3.52 Å from the kinked starting structure were observed. The study further concluded that, by using the PME method instead of a cutoff method, the fine structural features of DNA were accurately reproduced in the simulation (Duan et al., 1997).

A simulation study of the Hin-recombinase-DNA complex compared the Ewald summation method and the residue-based cutoff method with a cutoff radius of 10 Å (Komeiji and Uebayasi, 1999). The Ewald summation method produced a stable trajectory with an rms deviation of ~3 Å, and the cutoff method failed to achieve a stable simulation.

Nanosecond simulations of the decamer d(CCCCCTTTTT)$_2$ have been carried out using the AMBER and CHARMM energy functions and the Ewald summation technique (Feig and Pettitt, 1997). The investigation found that the CHARMM parameters gave an A-form DNA and that the AMBER parameters showed a B-DNA form in the first 3.5 ns and then transformed closer to the A-form DNA structure as found by the CHARMM parameters. From this observation, it was discussed that the AMBER parameters might need several nanoseconds to converge (Feig and Pettitt, 1997). These simulations were afterward extended, and the CHARMM parameters showed A-DNA base geometry and the purine strand was found in the A-DNA form, but the pyrimidine strand fluctuated between A and B forms (Feig and Pettitt, 1998). This investigation found B-DNA form for both the strands and an intermediate A- and B-DNA base geometry. In another paper focusing on ionic effects, the A-DNA form was obtained with the CHARMM parameters and the AMBER parameters preferred the B-DNA form (Feig and Pettitt, 1999).

A human prion protein model has been analyzed using molecular dynamics, in which the electrostatic interactions were handled in two different ways: the PME method and a truncation method with a cutoff radius of 8 Å (Zuegg and Gready, 1999). Several trajectories were generated with both methods, and the PME method showed, in all simulations, lower rms deviations than the cutoff method. The study concluded that correct treatment of the electrostatic interactions is important for proteins with large number of charged residues on the surface (Zuegg and Gready, 1999).

The validation and computational cost of the PME method in comparison with cutoff methods have been discussed (Darden et al., 1999). A recent review described the differences between various cutoff methods and Ewald summation methods (Cheatham and Brooks, 1999). A number of applications of the truncation methods and the advantages and disadvantages were also described. The PME method has been compared to the P^{3}M algorithm (Pollock and Glosli, 1996) for a box of water and the relative rms force errors were found to be quite similar (Darden et al., 1997). Three Ewald summation methods have also been thoroughly examined concerning accuracy differences (Deserno and Holm, 1998). Recently it has been argued that the Ewald summation method can be the standard of accuracy for calculating long-range electrostatic forces (Hermans, 1997).

Recently the artifacts in explicit solvent simulations of biological molecules using the Ewald method have been thoroughly analyzed using continuum electrostatics (Weber et al., 2000). In aqueous simulations of a polyalanine octapeptide, the P^{3}M method was applied to truncate the long-range interactions in three different sizes of the cubic unit cell. It was found that, in the largest unit cell, the peptide unfolds quickly as is experimentally expected, in contrast to the smaller unit cells in which severe artificial periodicities were observed. The study further argues that periodicity artifacts can be important in systems that include few hydration shells around the solute, solvent with low dielectric permittivity, and a solute with a large dipole or net charge (Weber et al., 2000).

In this report, we analyze the effects of a number of different truncation methods, which recently have been used to handle long-range electrostatic interactions in highly charged nucleic acids. The investigation was performed in a consistent way to allow a rigorous comparison between the truncation methods. As a model compound in this study, we focus on a right-handed double-stranded B-DNA hexamer solvated in aqueous solution.

TRUNCATION METHODS

To reduce the amount of time spent computing the large number of pairwise electrostatic interactions in a molecular dynamics simulation, it is common practice to neglect interactions beyond some cutoff distance, r_{off}. Such spherical cutoffs can be implemented in different ways, depending on whether the distance is calculated between the interacting atoms (atom-based) or between two groups of atoms (group-based). Furthermore, the interaction energy or force can be *truncated* abruptly at the cutoff distance, or some kind of smoothing scheme can be applied, either on the whole range $0 < r < r_{\text{off}}$ (a *shift*), or over a limited region $r_{\text{on}} < r < r_{\text{off}}$ (a *switch*). The shifting or switching function $S(r)$, as described below for the different cases, multiplies Coulombs law to give the effective form of the electrostatic interaction used in the calculations. In this section, the different truncation methods, which have been applied in this study to treat the long-range electrostatic interactions, are described. The shifting function (Brooks et al., 1983), which is usually used to shift the potential energy to zero, has the form,

$$S(r) = \begin{cases} (1 - (r/r_{\text{off}})^2)^2, & r \le r_{\text{off}} \\ 0, & r > r_{\text{off}}. \end{cases}$$

The shifting function increases the magnitude of the force before it is smoothed to zero. Short-range interactions of charged groups are distorted by the shifting function, and the short-range forces are overestimated (Loncharich and Brooks, 1989). A deeper and broader minimum has been observed for the shifting function compared to the no cutoff potential, and this caused overestimated atomic fluctuations for cutoffs shorter than 11.0 Å (Loncharich and Brooks, 1989).

In the range $r_{on} \le r \le r_{off}$ the switching function switches off the electrostatic interactions. The switching function (Brooks et al., 1983) is given by

$$S(r) = \begin{cases} 1, & r \le r_{on} \\ \dfrac{(r_{off}^2 - r^2)^2(r_{off}^2 + 2r^2 - 3r_{on}^2)}{(r_{off}^2 - r_{on}^2)^3} & r_{on} < r \le r_{off} \\ 0, & r > r_{off}. \end{cases}$$

This switching function can be applied to both atom- and group-based potentials and gives continuous force and potential energy. The dynamics of proteins has been observed to artificially decrease when the potential has been switched off over distances <4 Å (Loncharich and Brooks, 1989). Large forces and changes in the potential can occur at long distances if the switching region is as short as 2 Å.

In the force-shifting function (Brooks et al., 1985) the atom–atom force is offset from the Coulombic force at $r \le r_{off}$ and has the form

$$S(r) = \begin{cases} (1 - r/r_{off})^2, & r \le r_{off} \\ 0, & r > r_{off}. \end{cases}$$

For the group–group interactions, the short-range interactions of charged groups are distorted (Loncharich and Brooks, 1989). The size of the short-range forces is underestimated by the force-shift potential. The force-shift potential has been shown to give more accurate short-range structure of water compared to the shifting potential (Brooks et al., 1985). In a study of pure water, the force-shift function and Ewald summation gave good structural and dynamic properties, and the force-shifting function performed better than the potential shift method (Prevost et al., 1990).

The atom-based force-switching function (Steinbach and Brooks, 1994) gives accurate forces at short ranges and damps them monotonically to zero from r_{on} to r_{off}. To integrate the switched force, the potential energy is given by

$$V(r) = \begin{cases} cr_{off}^4(r^{-1} - r_{off}^{-1})\dfrac{(r_{off}^2 - 3r_{on}^2)}{(r_{off}^2 - r_{on}^2)^3} \\ \quad + 6cr_{on}^2r_{off}^2\dfrac{(r_{off} - r)}{(r_{off}^2 - r_{on}^2)^3} \\ \quad - c(r_{off}^3 - r^3)\dfrac{(r_{on}^2 + r_{off}^2)}{(r_{off}^2 - r_{on}^2)^3} + \dfrac{2c(r_{off}^5 - r^5)}{5(r_{off}^2 - r_{on}^2)^3} \\ \quad + 8cr_{on}^2r_{off}^2\dfrac{(r_{off} - r_{on})}{(r_{off}^2 - r_{on}^2)^3} - \dfrac{8c(r_{off}^5 - r_{on}^5)}{5(r_{off}^2 - r_{on}^2)^3}, & r \le r_{on} \\ \quad - \displaystyle\int_{r_{off}}^{r} S(r)F(r)\,dr, & r_{on} < r \le r_{off} \\ 0, & r > r_{off}, \end{cases}$$

where $S(r)$ is the switching function (see above), which switches off the force, $F(r)$. Artificial minima can occur when too short switching distances are used, but they are less pronounced than for the potential switching function (Steinbach and Brooks, 1994). Energy is conserved for the atom-based approach, but not for the group–group force-switching method (Steinbach and Brooks, 1994).

In the PME method (Darden et al., 1993), the slow summation is split into two faster summations that converge efficiently as $N \cdot \log(N)$. The electrostatic potential energy is defined as

$$E_{ele} = \frac{1}{2}\sum_{i=1}^{N}\sum_{j=1}^{N} q_iq_j \sum_{l=0}^{\infty}\sum_{m=0}^{\infty}\sum_{n=0}^{\infty}\frac{\mathrm{erfc}(\kappa|r_{ij} + a|)}{|r_{ij} + a|} - \frac{\kappa}{\sqrt{\pi}}\sum_{i=1}^{N} q_i^2 + \frac{1}{2}\sum_{i=1}^{N}\sum_{j=1}^{N}\frac{q_iq_j}{\pi L_xL_yL_z}\sum_{l=0}^{\infty}\sum_{m=0}^{\infty}\sum_{n=0}^{\infty} \times \frac{\exp(-|k|^2/4\kappa^2)\cos(k \cdot r_{ij})}{|k|^2} + J(D, \varepsilon'),$$

where erfc is the complementary error function; the first term is the real space summation; the second term is a correction for the self-energy of the canceling charge; the third term is the reciprocal space summation, which is truncated at an ellipsoidal boundary; and the fourth term is a surface correction term, which involves the unit cell dipole moment D and the surrounding dielectric constant ϵ' (Allen and Tildesley, 1987). The reciprocal space lattice vector is $k = 2\pi(l/L_x, m/L_y, n/L_z)$, a defines the lattice vector, and κ decides the relative rate of convergence. In the PME method, the complex exponentials in the reciprocal space summation are approximated using local Lagrange interpolation (Darden et al., 1993). More recently, the interpolation in the PME method was updated by incorporating Euler spline interpolation based on B-splines (Essmann et al., 1995). Standard implementations of the PME method assume periodic boundary conditions, but variants allowing also nonperiodic systems were described (Pollock and Glosli, 1996). This PME approach takes advantage of the smoothness of the B-splines. Recently, a review concerning the PME method was published (Sagui and Darden, 1999).

METHODOLOGY OF DNA SIMULATIONS

In this study, we focus on the right-handed double-stranded oligonucleotide $d(CGCGCG)_2$ in the B-DNA form. Earlier experimental and theoretical investigations focused on this hexamer (Borer et al., 1994; Norberg, 1995; Norberg and Nilsson, 1996b). X-ray fiber diffraction data were used to build the hexamer (Arnott et al., 1976). Ten sodium counterions were added to make the system electrically neutral. The counterions were placed on the bisector of the phosphate oxygens, 4.7 Å from the phosphorus atom, which was treated with full charge. The oligonucleotide and counterions were solvated in a 37.7-Å side length cubic box, which

was generated from TIP3P water molecules (Jorgensen et al., 1983). To remove bad contacts, the water molecules were energy minimized 200 steps of steepest descent while the hexamer was constrained using a harmonic potential with a force constant of 20.0 kcal·mol^{-1}·Å^{-2}. Periodic boundary conditions were applied throughout the molecular dynamics simulations, which were carried out at 300 K. The leap-frog algorithm (van Gunsteren and Berendsen, 1990) was used for the integration of the equations of motion. To be able to apply a time step of 0.002 ps, the hydrogen atom-heavy atom bond lengths were constrained using the SHAKE algorithm (Ryckaert et al., 1977). A relative dielectric constant of 1.0 was applied and the nonbonded list was updated every 20 steps. The coordinates from the different trajectories were saved every 0.5 ps. Both the energy minimizations and molecular dynamics simulations were performed with the CHARMM program (Brooks et al., 1983) and the all-atom version 27 parameters (Foloppe and MacKerell et al., 2000). The differences between these parameters and the all-atom version 22 parameters (MacKerell et al., 1995) will be discussed.

In all the simulations, the van der Waals interactions were treated in the same manner using a shifting function (Brooks et al., 1983), which damped the force monotonically to zero. The focus in this investigation is on the long-range electrostatic interactions, for which we applied eleven different truncation methods as displayed in Table 1. These are:

1. the atom-based approach using the shifting function (Brooks et al., 1983) and a cutoff of 12.0 Å (defined as ASH),
2. the atom-based approach with the force-shift method (Brooks et al., 1985) and a short cutoff of 8.0 Å (AFSHS),
3. the atom-based approach with the force-shift method (Brooks et al., 1985) and a cutoff of 12.0 Å (AFSH),
4. the atom-based approach and the force-shift method (Brooks et al., 1985) with a long cutoff of 18.0 Å (AFSHL),
5. the atom-based approach and a force-switching function (Steinbach and Brooks, 1994), which was turned on at 8.0 Å and turned off at 12.0 Å (AFSW),
6. the atom-based approach and a potential-switching function (Steinbach and Brooks, 1994), which was turned on at 8.0 Å and turned off at 12.0 Å (ASW),
7. the particle-mesh Ewald method (Essmann et al., 1995) (PME),
8. the group-based approach with a switching function (Steinbach and Brooks, 1994), which was turned on at 8.0 Å and turned off at 12.0 Å (GSW) and
9. the group-based approach and a force-switching function (Steinbach and Brooks, 1994), which was turned on at 8.0 Å and turned off at 12.0 Å (GFSW).
10. the group-based approach with a direct and abrupt truncation at 8.0 Å (GTRS)
11. the group-based approach and a direct and abrupt truncation at 12.0 Å (GTR).

The parameters, for instance, the grid spacing and the direct cutoff, in the PME method have not been optimized for computational efficiency. In the PME simulation, the direct space nonbonded calculations were truncated using a 12.0 Å cutoff and a sixth-order interpolation scheme was used with 32 grid points in each direction for the fast Fourier transformation. κ was set to 0.34.

To accomplish a consistent and careful comparison between the different truncation methods, all the simulations were carried out in the same way. The simulations were performed on a PC cluster of 450 MHz Pentium II nodes running Linux. The nodes were connected using a Fast Ethernet switch. In the simulations, we first equilibrated the B-DNA systems during 30 ps using constant pressure with a coupling constant of 1.0 ps^{-1} (Berendsen et al., 1984). Thereafter, the eleven simulations were extended in the NVE ensemble for 500 ps giving a total of 530 ps. The AFSH and PME truncation methods have been applied in a number of MD studies (see Introduction), and, therefore, these simulations were further extended to 5.03 ns. The analysis of the 500-ps simulations was carried out for the

TABLE 1 Truncation methods for long-range electrostatic interactions

Method	Molecular Part for Cutoff	Cutoff (Å)	Scheme
Shifting function	Atom-based	12.0	ASH
Force-shifting function	Atom-based	8.0	AFSHS
Force-shifting function	Atom-based	12.0	AFSH
Force-shifting function	Atom-based	18.0	AFSHL
Force-switching function	Atom-based	8.0–12.0	AFSW
Switching function	Atom-based	8.0–12.0	ASW
Particle-mesh Ewald	Atom-based		PME
Switching function	Group-based	8.0–12.0	GSW
Force-switching function	Group-based	8.0–12.0	GFSW
Truncation	Group-based	8.0	GTRS
Truncation	Group-based	12.0	GTR

last 200 ps and for the 5.03-ns simulations the last 1.0 ns. Only small differences in the values were obtained when the analysis period was changed. The rms deviations from A- and B-DNA were calculated with the ideal A- and B-DNA as reference structures, and are therefore slightly larger than if energy minimized A- and B-DNA forms had been used.

RESULTS AND DISCUSSION

To obtain accurate molecular dynamics simulations on the nanosecond time scale or beyond of nucleic acids, one has to carefully treat the long-range interactions, which are important for the structural stability and dynamic behavior. Recently, a number of studies have claimed to have obtained very stable and accurate nanosecond molecular dynamics simulations as discussed above (see Introduction). Here, we report the results from a comparison of the most commonly used truncation methods, which have been applied to treat the long-range interactions in biological systems.

Two simulations, which used the group-based approach with abrupt truncation at a long and a short cutoff radius, were performed. The rms deviations from the starting conformation are displayed in Fig. 1.

In the GTRS simulation, the rms deviation increased dramatically during the first 300 ps and caused considerable divergence from the initial structure. These severe distortions were mainly due to the too short cutoff of 8 Å, which was applied in the simulation. In the other case, then, the cutoff radius was extended to 12 Å a stable trajectory was found. A heavy-atom rms deviation of 2.5 Å was found in the GTR simulation, which was nearly 1 Å larger compared to several of the other truncation methods (Table 2).

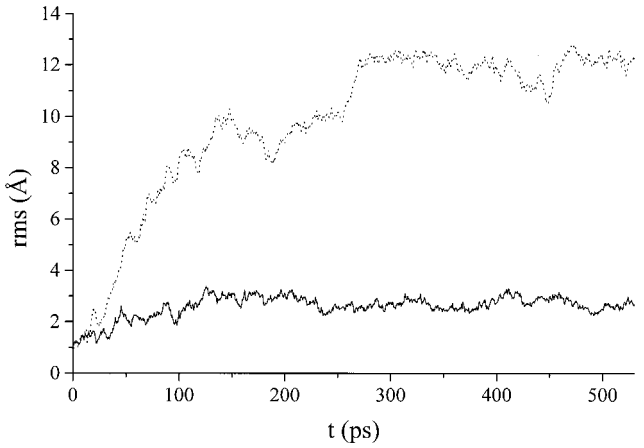

FIGURE 1 Root mean square atomic deviations as a function of time from the initial structure for all heavy atoms of the hexamer using the group-based truncation (GTRS) method with a cutoff of 8.0 Å (· · · · · ·) and the group-based truncation (GTR) method with a cutoff of 12.0 Å (——).

TABLE 2 Deviations in rms (Å) of the B-DNA hexamer, bases, and backbone for heavy atoms and all atoms average over the last 200 ps

Truncation Scheme	Atoms	Heavy Atoms	All Atoms
ASH	Hexamer	1.66 (0.29)	1.82 (0.30)
	Bases	1.26 (0.25)	1.35 (0.27)
	Backbone	1.88 (0.34)	2.04 (0.35)
AFSHS	Hexamer	1.71 (0.27)	1.94 (0.26)
	Bases	1.08 (0.20)	1.17 (0.20)
	Backbone	2.10 (0.33)	2.33 (0.31)
AFSH	Hexamer	1.53 (0.24)	1.74 (0.24)
	Bases	0.98 (0.17)	1.05 (0.17)
	Backbone	1.84 (0.30)	2.08 (0.30)
AFSHL	Hexamer	1.57 (0.19)	1.77 (0.20)
	Bases	1.02 (0.12)	1.08 (0.12)
	Backbone	1.88 (0.25)	2.11 (0.26)
AFSW	Hexamer	1.75 (0.22)	1.92 (0.24)
	Bases	1.34 (0.20)	1.45 (0.21)
	Backbone	1.96 (0.25)	2.14 (0.27)
ASW	Hexamer	1.04 (0.02)	1.21 (0.02)
	Bases	0.69 (0.02)	0.78 (0.03)
	Backbone	1.24 (0.02)	1.42 (0.03)
PME	Hexamer	1.48 (0.24)	1.65 (0.25)
	Bases	1.08 (0.15)	1.15 (0.15)
	Backbone	1.70 (0.31)	1.90 (0.32)
GSW	Hexamer	4.43 (0.13)	4.58 (0.11)
	Bases	4.89 (0.16)	5.15 (0.15)
	Backbone	3.66 (0.09)	3.81 (0.09)
GFSW	Hexamer	3.27 (0.22)	3.57 (0.22)
	Bases	2.42 (0.23)	2.58 (0.23)
	Backbone	3.86 (0.24)	4.14 (0.23)
GTRS	Hexamer	11.77 (0.44)	11.94 (0.45)
	Bases	12.35 (0.59)	12.59 (0.58)
	Backbone	10.76 (0.48)	11.03 (0.51)
GTR	Hexamer	2.54 (0.19)	2.70 (0.22)
	Bases	2.84 (0.25)	3.04 (0.30)
	Backbone	2.10 (0.21)	2.30 (0.24)

Standard deviations are shown in parenthesis.

Another way to truncate the long-range electrostatic interactions instead of abrupt truncation is to use a switching function (see Truncation methods). Figure 2 shows rms deviation obtained from the B-DNA simulations in which the ASW, GSW, or GFSW truncation methods handled the long-range electrostatic interactions. In the 500-ps simulations with the group-based approaches, quite large rms deviations ~3–4 Å were found. Concerning the GFSW simulation, the rms deviation increased until 360 ps, whereafter only a slight increase in the rms deviation was observed. For the GFSW truncation method, the rms deviation of the heavy atoms for the last 200 ps was 3.27 Å. In the case of the GSW simulation, the rms deviation leveled out after 75 ps. Both the group-based approaches showed significant divergences, ~3–4 Å from the initial structure. Similar observations have been made in other studies, for instance, simulations of the $d(CCAACGTTGG)_2$ decamer showed rms deviations >4 Å when a charge group-based truncation method with and without evaluation of all solute–solute interactions were applied (Cheatham et al., 1995). In

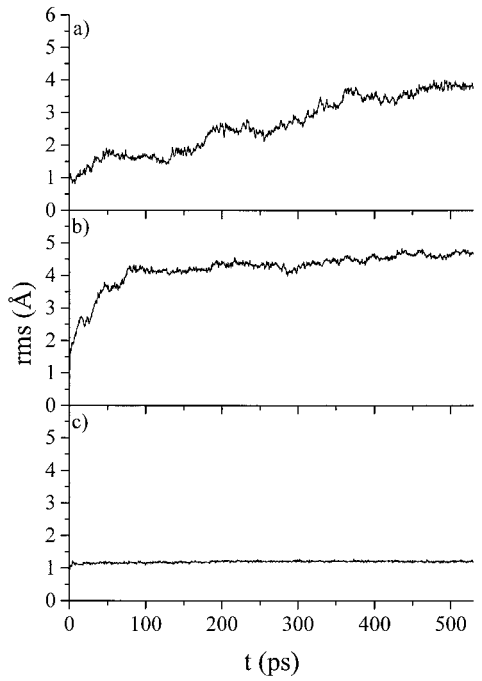

FIGURE 2 Root mean square atomic deviations versus time from the initial B-DNA structure for all heavy atoms of the hexamer using the truncation schemes (*a*) group-based force-switching function (GFSW), (*b*) group-based switching function (GSW), and (*c*) atom-based switching function (ASW).

a vacuum MD study of myoglobin, the largest rms deviations occurred when using group–group truncation methods compared to atom–atom truncation methods (Loncharich and Brooks, 1989). Another study of myoglobin in aqueous solution has also shown that the worst results are obtained by the group-based potential truncation (Steinbach and Brooks, 1994).

A simulation was also performed using the switching function and the atom-based, instead of group-based, approach. It is immediately obvious from Fig. 1 that the hexamer becomes very rigid in the ASW simulation, due to the large forces introduced by the switching function, at distances in the switching region (Loncharich and Brooks, 1989; Steinbach and Brooks, 1994).

For the ASH truncation method, the trajectory was found to be quite stable during the 500-ps simulation (Fig. 3 *b*). At the end of the simulation, the rms deviation increased slightly, and a value of 1.66 Å was obtained during the last 200 ps. This confirmed that the B-DNA form was well preserved in the simulation. For the AFSW simulation, a marginally larger rms deviation compared to the ASH simulation was obtained, but slightly smaller rms fluctuations. Overall, both simulations showed stable trajectories, with the bases less mobile than the backbone.

In a number of previously reported simulations, the atom-based approach with the force-shifting function was applied (Norberg, 1995; Norberg and Nilsson, 1995). These nucleic acid simulations showed accurate and very stable trajectories of dinucleoside monophosphates with low rms deviations of ~1 Å, but also for oligonucleotides. Potential of mean force calculations of dinucleoside monophosphate showed that stacking and thermodynamic properties are well behaved, and comparison with NMR relaxation data also showed that the dynamic properties are well reproduced (Norberg and Nilsson, 1995, 1996c).

In the present study, this truncation method was applied together with three different cutoff radii, 8 Å, 12 Å and 18 Å. This was done to investigate how the cutoff radius affected the accuracy of the simulation and to illustrate the computational effort required. For the AFSHS simulation with a cutoff radius of 8 Å, the hexamer conformation was maintained well throughout the simulation (Fig. 3 *A*). The rms deviations were 1.08 and 2.10 Å for the bases and backbone, respectively. When the cutoff radius was increased from 8 to 12 Å in the AFSH simulation, the heavy-atom rms deviation decreased from 1.71 to 1.53 Å, and both the bases and backbone in the AFSH simulation were closer to the initial conformation. Usually a spherical cutoff of 10–12 Å is applied to truncate the long-range electrostatic interactions, and Steinbach and Brooks (1994) recommend the use of a 12-Å or longer cutoff. In a few cases, longer cutoff radii have been used, for instance, in a protein crystal simulation, a 25.0-Å cutoff was used (Kitson et al., 1993). Here, we also applied a longer cutoff radius of 18 Å to address the question of optimal accuracy in a solution simulation. A heavy-atom rms deviation of 1.57 Å was obtained for the AFSHL simulation (Table 2). This showed that the rms deviations were very similar for the force-shifting function with cutoffs of 18 and 12 Å. A slight decrease of the rms fluctuations with increasing cutoff radius was observed. The rms deviation was improved with 0.2 Å by going from a cutoff of 8 to 12 Å, but a further increase of the cutoff radius to 18 Å did not show any significant difference.

A number of recent MD studies have successfully applied the PME method to treat the long-range interactions as previously discussed (see Introduction). Here, we wanted to do a complete comparison between available truncation algorithms. For the PME method, an rms deviation of 1.48 Å was obtained, which is slightly lower, but not significantly, than for the AFSH simulation. The bases of the hexamer exhibited larger rms deviation for the PME method compared to the AFSH and AFSHL simulations, but, for the backbone, the reverse was observed (Table 2). Therefore, the PME method seemed to reduce the mobility of the highly charged backbone. Still the rms fluctuations were quite similar for the AFSH and PME methods.

A previous study performed a stable 400-ps trajectory of the double-stranded riboguanylyl-3′,5′-ribocytidine using the PME method (Lee et al., 1995). The study reported an rms deviation of 1.02 Å for the heavy atoms. Accurate

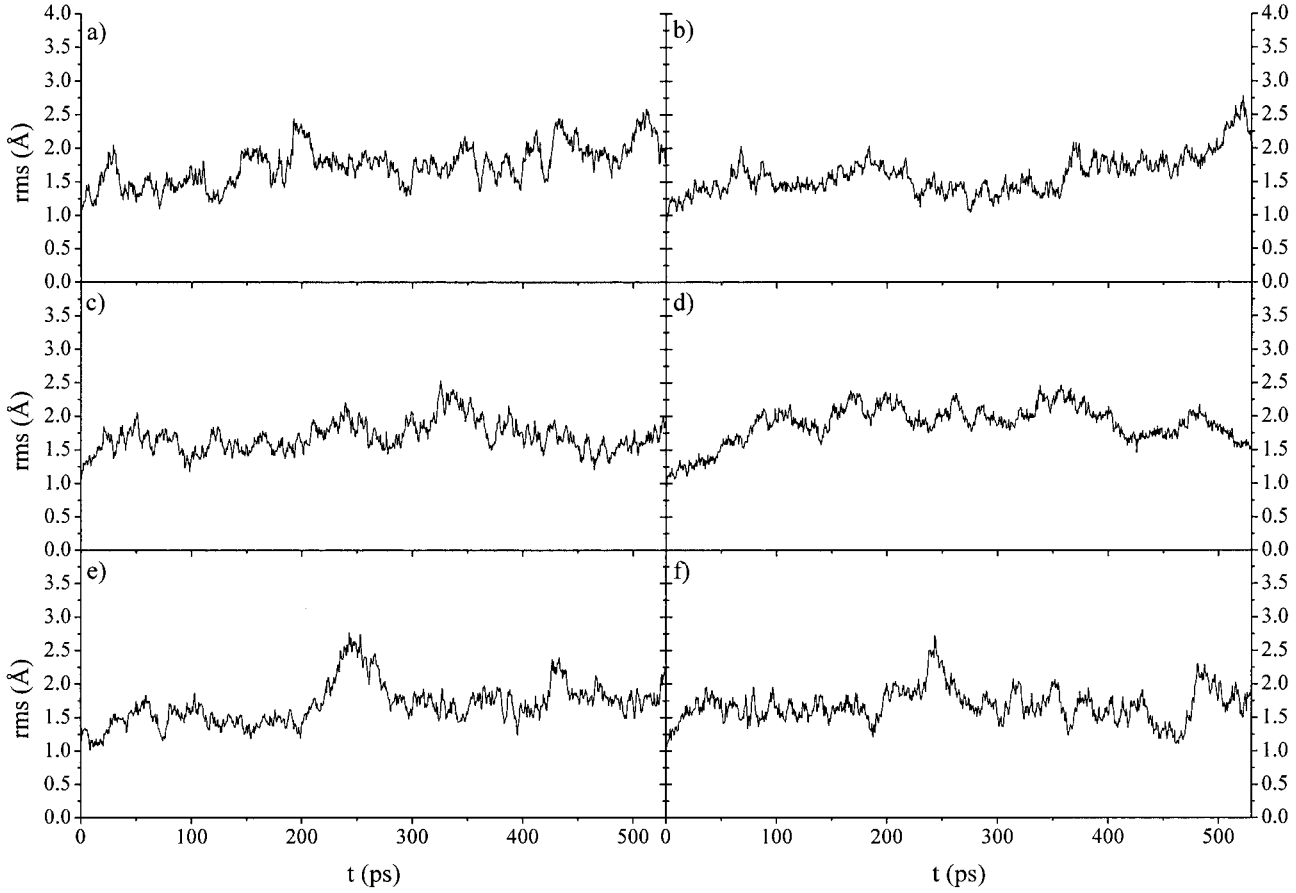

FIGURE 3 Root mean square atomic deviations as a function of time from the initial B-DNA structure for all heavy atoms of the hexamer using the following truncation methods: (*a*) the atom-based force-shifting function with a cutoff of 8.0 Å (AFSHS); (*b*) the atom-based shifting function with a cutoff of 12.0 Å (ASH); (*c*) the atom-based force-shifting function with a cutoff of 12.0 Å (AFSH); (*d*) the atom-based force-switching function with a switching region of 8.0–12.0 Å (AFSW); (*e*) the atom-based force-shifting function with a cutoff of 18.0 Å (AFSHL); and (*f*) the particle mesh Ewald method (PME).

simulations using the atom-based approach with a force-shifting function have also been carried out for the riboguanylyl-3′,5′-ribouridine dimer using various boundary conditions, parameter sets, water models, and different ensembles (Norberg and Nilsson, 1995). In the investigation of the riboguanylyl-3′,5′-ribouridine dimer, all-atom rms deviations between 0.80 and 1.27 Å were obtained. The influence of pressure was analyzed for the same RNA fragment and the all-atom rms deviations were in the 1.18–1.26 Å range (Norberg and Nilsson, 1994). In another MD study, the riboadenylyl-3′,5′-riboadenosine dimer showed stable trajectories in aqueous solution and also in organic solvents, but with higher mobility, using the atom-based approach with the force-shifting function (Norberg and Nilsson, 1998). The atom-based approach with the force-shifting function has previously been applied to a pentamer and a hexamer in aqueous solution (Norberg and Nilsson, 1996b). In these stable simulations, the heavy-atom rms deviations were 2.24 Å and 2.52 Å, respectively (Norberg and Nilsson, 1996*b*). This demonstrated that, with longer DNA molecules, larger rms deviations would be expected. An investigation has also found stable trajectories for DNA and RNA dodecamers when the atom-based approach with the force-shifting function was used (Norberg and Nilsson, 1996a). The DNA dodecamer from the *Eco*RI recognition site has been simulated in different salt concentrations, and the study found stable trajectories using the atom-based approach with a shifting function (MacKerell, 1997). In the present 500-ps simulations, the rms deviations of 1.5–1.7 Å for the heavy atoms are at least on the same level as those of other nucleic acid MD solution studies (see Introduction). The investigations mentioned above and the present one clearly demonstrate that the atom-based approach with a shifting function or a force-shifting function give stable trajectories of nucleic acids. Several studies (Kitson et al., 1993; Lee et al., 1995; York et al., 1995) claim that accurate MD simulations have been obtained when focusing on the biomolecule in its crystal environment, a situation which should be distinguished from accurate solution MD studies. It is clearly two different subjects to simulate a biomolecule

in solution or in its crystal environment. A recent study carried out both crystal and solution simulations of a decamer and showed that rms deviations are ~1.0–1.5 Å for crystal simulations and in the range 3.6–4.2 Å for solution simulations (Bevan et al., 2000). For instance, the $d(CGCGAATTCGCG)_2$ dodecamer was simulated both in solution and in its crystal environment (Miaskiewics et al., 1996; York et al., 1995) using the AMBER program with the second generation all-atom parameters (Cornell et al., 1995) and the PME method. The reported heavy-atom rms deviations from the starting structure were 1.16 Å in its crystal environment (Miaskiewics et al., 1996) and 2.5 Å in solution (York et al., 1995). In another investigation, the force-shift function was used to develop nucleic acids parameters, but also to demonstrate that accurate and stable trajectories were generated (Langley, 1998). All published rms deviations from the initial structure of biological molecules in solution are clearly larger than the corresponding values obtained in the crystal environment. One can also notice that a number of studies prefer to report heavy-atom rms deviations of the whole molecule, or, for instance, the recognition site and not the all-atom rms deviations. The studies mentioned above and the one reported here clearly show that different truncation methods can be applied to obtain accurate and stable simulations of biological molecules.

To further investigate and understand the level of the accuracy and stability of the trajectories on the nanosecond time scale, the simulations using the AFSH truncation method and the PME method were further extended to 5.03 ns. The AFSH simulation was chosen because the AFSHL truncation method showed no improved accuracy and was substantially more expensive (see below).

In Fig. 4, the time evolution of the heavy-atom rms deviations from the initial B-DNA structure during 5030 ps

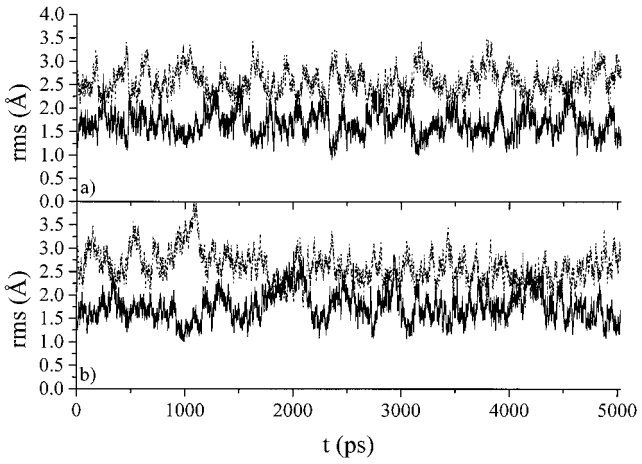

FIGURE 4 Root mean square atomic deviations versus time from the initial ideal B-DNA structure (——) and from the ideal A-DNA structure (·····) for all heavy atoms of the hexamer in the extended 5030-ps simulations using (*a*) the PME and (*b*) the AFSH methods.

are displayed for the AFSH and PME simulations. For the extended simulation using the AFSH truncation method, we found a heavy-atom rms deviation of 1.61 Å from the initial structure (Table 3). This value is slightly larger than the heavy-atom rms deviation found after 500 ps. A similar behavior was also seen in the PME simulation, which had a heavy-atom rms deviation of 1.52 Å. For both the AFSH and PME simulations, the heavy-atom rms deviations of the bases were 1.1 Å. About 0.6–0.7-Å larger rms deviations were obtained for the backbone. A B-DNA conformation was observed for both the bases and the backbone. The rms fluctuations are clearly larger for the backbone than for the bases with both methods. In another MD study of the $d(CGCGAATTCGCG)_2$ dodecamer, higher rms fluctuations were found for the three base pairs at the ends, ~1.5 Å, compared to the central four A:T base pairs, ~0.8 Å (Duan et al., 1997).

The time evolution of the heavy-atom rms deviations from the A-DNA form of the studied hexamer for both the AFSH and PME simulations are shown in Fig. 4. The heavy-atom rms deviation from the A-DNA form of the initial hexamer was ~2.28 and ~2.36 Å for the AFSH and PME simulations, respectively (Table 3). An rms difference of ~6.5 Å distinguishes the canonical A-DNA form from the B-DNA. The generated MD trajectories for both truncation methods showed to be closer to the B-DNA initial structure than to the A-DNA form. A heavy-atom rms deviation of ~1.9 Å from the A-DNA form for the bases was observed in both the AFSH and PME simulations. For the backbone, the heavy-atom rms deviation was ~2.5–2.6 Å. By starting from a B-DNA form of the hexamer and using either the AFSH or the PME truncation method, the B-DNA conformation was maintained throughout the simulations with the CHARMM version 27 parameters (Foloppe and MacKerell, 2000). We also simulated the $d(CGCGCG)_2$ duplex with the CHARMM version 22 parameters (MacKerell et al., 1995) and the different truncation methods, and the results (data not shown) are very consistent with our present results, except that the structures obtained with the well behaved methods were A-DNA like.

Conformational transitions have been found by others, for instance, a B-to-A transition was observed for the $d(CGCGAATTCGCG)_2$ dodecamer using the CHARMM version 22 parameters and the Ewald method (Yang and Pettitt, 1996). The same dodecamer was also studied in different salt concentrations using the CHARMM version 22 parameters and the potential shifting function (MacKerell, 1997). In all of the simulations, an A-DNA form of the dodecamer was obtained. MD simulations of a dodecamer in the B-DNA form were carried out using the CHARMM version 22 parameters and a transition to the A-form was observed (Norberg and Nilsson, 1996a). In a simulation study of the $d(CCCCCTTTTT)_2$ decamer, both the AMBER and CHARMM parameters were used, and the Ewald technique was used (Feig and Pettitt, 1997). The

TABLE 3 Deviations in rms (Å) of all heavy atoms and all atoms from A-DNA form and from B-DNA starting conformation of the hexamer for the AFSH and PME simulations extended to 5030 ps and average over the last 1000 ps

Cutoff Method	DNA Form	Atoms	Bases	Backbone	Hexamer
AFSH	A-DNA	heavy	1.86 (0.25)	2.54 (0.35)	2.28 (0.28)
	A-DNA	all	1.97 (0.25)	2.77 (0.34)	2.48 (0.28)
AFSH	B-DNA	heavy	1.13 (0.21)	1.88 (0.42)	1.61 (0.33)
	B-DNA	all	1.20 (0.21)	2.06 (0.42)	1.78 (0.34)
PME	A-DNA	heavy	1.89 (0.23)	2.66 (0.31)	2.36 (0.25)
	A-DNA	all	2.00 (0.23)	2.87 (0.30)	2.56 (0.26)
PME	B-DNA	heavy	1.11 (0.21)	1.74 (0.33)	1.52 (0.28)
	B-DNA	all	1.19 (0.22)	1.92 (0.33)	1.69 (0.28)

Standard deviations are shown in parenthesis.

study found an A-DNA structure in the 4.0-ns simulation using the CHARMM parameters and a more B-DNA-like conformation using the AMBER parameters in the first 3.5 ns, but, at ~4.0 ns, the conformation had been transformed to a more A-DNA-like form (Feig and Pettitt, 1997). A conformation slightly closer to the B-DNA form was observed for the $d(CCAACGTTGG)_2$ decamer using the AMBER parameters and the PME method (Cheatham and Kollman, 1996). In another study, a comparable observation of a slightly more B-form-like dodecamer was seen while using the AMBER parameters and the PME truncation method (Cieplak et al., 1997).

As a comparison, the A-DNA and B-DNA form of the studied hexamer side by side with the average structures obtained from the simulations using the AFSH truncation method and the PME method are displayed in Fig. 5. The present study and the discussed investigations clearly demonstrate a B-DNA form using the CHARMM version 27 parameters for both the bases and the backbone. Previously, an A-DNA form was obtained using the version 22 parameters (Norberg and Nilsson, 1996a). A B-DNA form, or for several nanosecond simulations a more A-DNA like form, has been observed using the AMBER 95 parameters (Feig and Pettitt, 1997). The AMBER 95 parameters have been modified to give more pronounced B-DNA and A-RNA conformations with more realistic sugar puckering and helical repeats, but then the previously seen B- to A-DNA transition in the presence of $Co(NH_3)_6^{3+}$ ions has been lost (Cheatham et al., 1999). Nucleic acid parameters have also been developed that reproduce both environmental and sequence-dependent effects of DNA structures (Langley, 1998). These observations are irrespective of which long-range truncation method that has been applied. Instead, the conformational transitions between A-DNA and B-DNA seem primarily to depend on the parameters of the energy function.

In Fig. 6, the mean square fluctuations for the atom-based force-shift and the particle mesh Ewald methods are displayed. In all the simulations, the four nonterminal base pairs showed smaller mean square fluctuations than the terminal base pairs. Concerning the terminal nucleotides, the cytidines were found to be more flexible than the guanosines. Among the nonterminal nucleotides, the mean square fluctuations were observed to be quite similar for both cytidines and guanosines. In the 5.03-ns simulations the mean square fluctuations were slightly larger for the AFSH method than for the PME method (Fig. 6 *a*). This was found for both the terminal and nonterminal nucleotides. For the AFSHS, AFSH, AFSHL, and PME simulations of 500 ps, the mean square fluctuations were compared (Fig. 6 *b*). A very similar pattern of the mean square fluctuations was observed for the different truncation methods. The mean square fluctuations were not affected by the changes of cutoff radius for the atom-based force-shift method. Both the PME method and atom-based force-shift methods showed mean square fluctuations of the same level. Similar observations with quite stable nonterminal base pairs and more flexible terminal base pairs have been reported for dodecamers composed of alternating G:C and C:G base pairs (Norberg and Nilsson, 1996a).

In a previous study, the distribution of phosphorus–phosphorus distances from a simulation of a B-DNA dodecamer was compared with the distribution found from a large number of x-ray crystal structures (Auffinger and Westhof, 1998). An artifactual peak at 8.5 Å was observed, and this was generated due to the use of the switching function for truncation. Probably the occurrence of this artifact depended on the very narrow switching range, just 1 Å between r_{on} and r_{off}. This artifact was not obtained in any of the simulations presented here, where a 4-Å range was used for the switching function. The distributions of the phosphorus–phosphorus distances for the AFSHS, AFSH, and AFSHL methods are displayed in Fig. 7 *a–c*. In the AFSHS and AFSH simulations, a peak at ~7 Å was found and a small tendency for a second peak ~6 Å. Two more pronounced and distinguishable peaks between 6 and 7 Å were found in the AFSHL simulation. The phosphorus–phosphorus distributions are more rugged for the 500-ps simulations than for the 5.03-ns simulations, because of better equilibration and better statistics in the 5.03-ns simulations. In these long simulations with the AFSH and the PME methods, the phosphorus-phosphorus distance distributions were

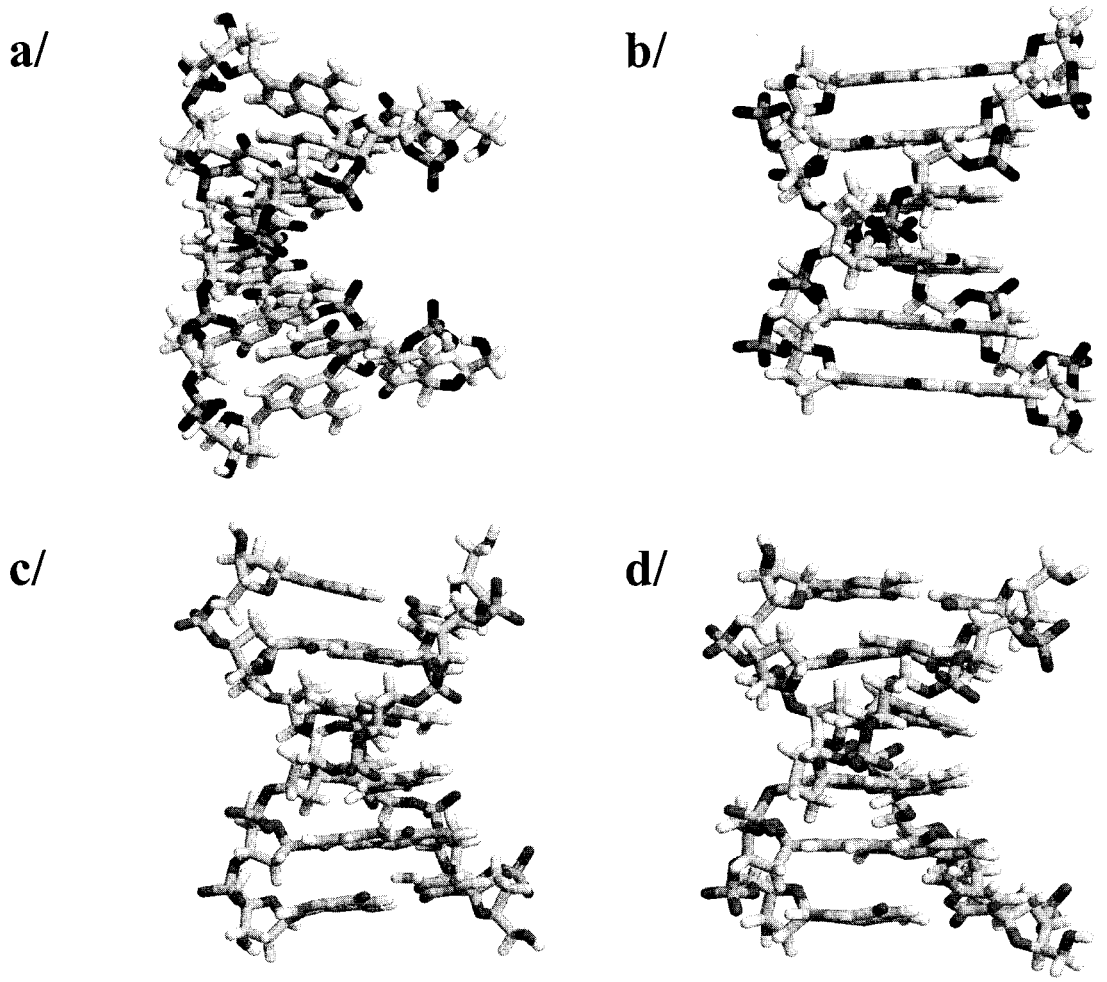

FIGURE 5 Structures of (*a*) A-DNA and (*b*) B-DNA forms and snapshots taken at 5.03 ns of the simulations, in which the (*c*) AFSH and (*d*) PME methods were applied.

quite similar (Fig. 7, *d* and *f*). For all the atom-based force-shift and PME simulations, the distribution curves showed a peak at 13 Å, which is the interstrand phosphate–phosphate distance, and at 18.5 Å. The artifactual peak observed at 8.5 Å was probably attributed to the use of a switching function with a very narrow range, r_{on} = 7.5 Å and r_{off} = 8.5 Å, for the switch (Auffinger and Westhof, 1998). In the present simulations, this peak was not seen. Here, the switch, when used, was applied over a 4-Å range starting at 8 Å, but, nevertheless, there is a clear relationship between the character of the P–P distance distributions (Fig. 7) and the structural rms deviations (Figs. 1, 2, and 3). The stable simulations (AFSH, AFSHS, AFSHL, ASH, PME, AFSW, and GTR) all have very similar P–P distance distributions, which resemble the data from crystal structures with peaks around 7, 13, and 18 Å (Auffinger and Westhof, 1998), in contrast to the simulations with large rms deviations where additional and shifted peaks (GSW, GFSW) or a general broadening (GTRS) occur. The peak at 7 Å, due to neighboring phosphorus atoms in the same DNA strand, was in the AFSHL simulation found to be split due to a base-dependent difference: the P–P distance was shorter when the base between the phosphorus atoms was a cytosine; this tendency is visible also in the 0.5-ns AFSH and PME simulations, but not in the 5-ns AFSH and PME simulations, indicating that it may have been a transient, metastable state. The atom-based switch (ASW) shows a large number of very sharp peaks in the P–P distance distributions, a reflection of the rigidity in the structure resulting from large forces introduced in the 4-Å-wide range of the switching function; it is therefore not surprising that the rms deviation in this simulation remained ~1 Å, with only very small fluctuations.

Knowledge about the computational resources required to perform a specific length of simulation is of great interest. Therefore, the time for carrying out a 1-ps simulation was determined for the different truncation methods using 1, 2, 4, and 8 computer nodes on a 450 MHz Pentium II-based

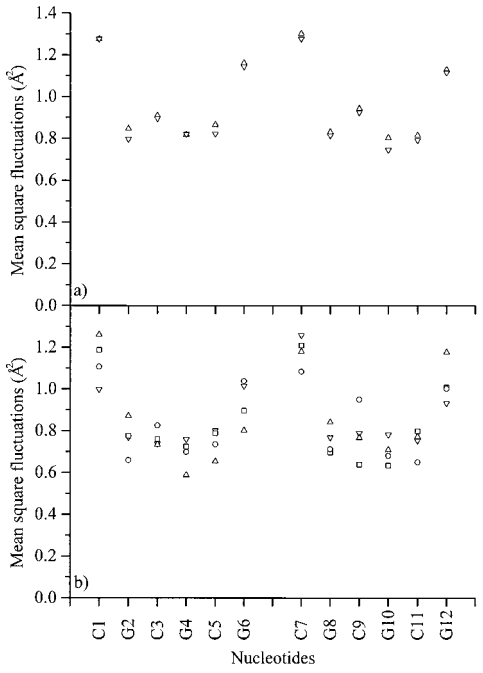

FIGURE 6 Mean square fluctuations of the heavy atoms for the (*a*) AFSH (*triangle*) and PME (*inverted triangle*) simulation of 5.03 ns and for the (*b*) AFSHS (*inverted triangle*), AFSH (*square*), AFSHL (*triangle*), and PME (*circle*) simulations of 500 ps.

cluster. Independent of the number of computer nodes, the group-based truncation methods were found to be faster than the atom-based methods. An extension of the cutoff radius from 8 to 12 Å for the atom-based force-shift method increased the required computational time 2.3 times for a single node and 1.6 times for 8 processors (Table 4). For a single processor, the AFSHL simulation was 6.4 times slower than the AFSH simulation, but only 3.3 times when 8 processors were used. By increasing the cutoff radius from 12 to 18 Å, the computational time increased 2.7 and 2.1 times for 1 and 8 nodes, respectively. For longer cutoffs, it becomes more efficient to use a larger number of nodes. Because the PME method has been shown to produce accurate and stable trajectories (see Introduction), it is of interest to compare its computational time with other truncation methods. For a single node, the PME simulation was 3.6 and 1.5 times slower than the AFSHS and AFSH simulations, respectively, but 1.8 times faster than the AFSHL simulation. When, instead, 8 processors were used, the AFSH and the AFSHS simulations were ~1.5 and 2.4 times faster than the PME simulation. In the atom-based force-shift method, a cutoff radius of ~14.5 Å demanded the same computational time as the PME method with a cutoff of 12.0 Å for the direct space nonbonded calculations. If the direct space nonbonded cutoff is reduced, the PME method becomes competitive concerning speed in comparison with the AFSH simulation. For comparison, the same system was also simulated using the AFSH truncation scheme in an 18 Å radius sphere of water, which fits just inside the cubic box used for the other simulations. The spherical system contained just 593 water molecules, for a total of 2165 atoms compared to 4985 in the periodic systems; because, in the spherical system, no image atoms have to be taken into account, the simulation is substantially faster than the other systems using a 12-Å cutoff: 5–7 times on one node, and 3–5 times on 8 nodes. At the same time, we noted that the structural (rms deviation of ~1.7 Å from B-DNA) and dynamic (mean square fluctuations of ~0.8 Å^2) properties of the DNA were virtually the same in the spherical system as in the well-behaved periodic systems.

CONCLUSIONS

In this report, we demonstrate that stable trajectories of biological molecules can be obtained using different methods to handle the long-range electrostatic interactions; for instance, the PME method or spherical cutoff methods such as the atom-based approach and a potential shifting function, a force-shifting function or a force-switching function. In the case of the group-based truncation methods, accurate and stable trajectories could not be obtained; instead, large rms deviations and structural distortions were seen for the hexamer. In a previous study of nucleic acid fragments, the atom-based approach and the force-shifting function was shown to give stable trajectories in both aqueous and organic solvents (Norberg and Nilsson, 1998). By increasing the cutoff from 8.0 to 12.0 Å for the atom-based approach with the force-shifting function, the rms deviations were observed to decrease ~0.2 Å. A further increase from a cutoff of 12 to 18 Å did not provide any significant increase of stability. In the present analysis of the hexamer, the deviations of the bases were found to be more restricted than the backbone as seen from the heavy-atom rms deviations (Tables 1 and 2). From the nanosecond simulations, the rms deviation from the initial structure was found to be very similar for the AFSH truncation method compared to the PME method. From these observations, we could not see that the PME method provides any improvement in accuracy or stability compared to, for instance, the ASH or the AFSH truncation methods.

Furthermore, we found that the nonterminal nucleotides were less mobile than the terminal nucleotides. The terminal cytidines were significantly more flexible than the terminal guanosines, indicating stronger base-stacking tendencies for the guanine base compared to the cytosine base as has previously been shown for deoxyribodinucleoside monophosphates (Norberg and Nilsson, 1996c). This dynamic behavior was observed for all of the truncation methods, for which stable trajectories were obtained.

In the 300–500-ps range, the rms deviation was 1.5 Å for both the AFSH and PME simulations. These simulations were further extended to 5.03 ns and showed, during the last 1.0 ns, rms deviations of 1.61 and 1.52 Å for the AFSH and

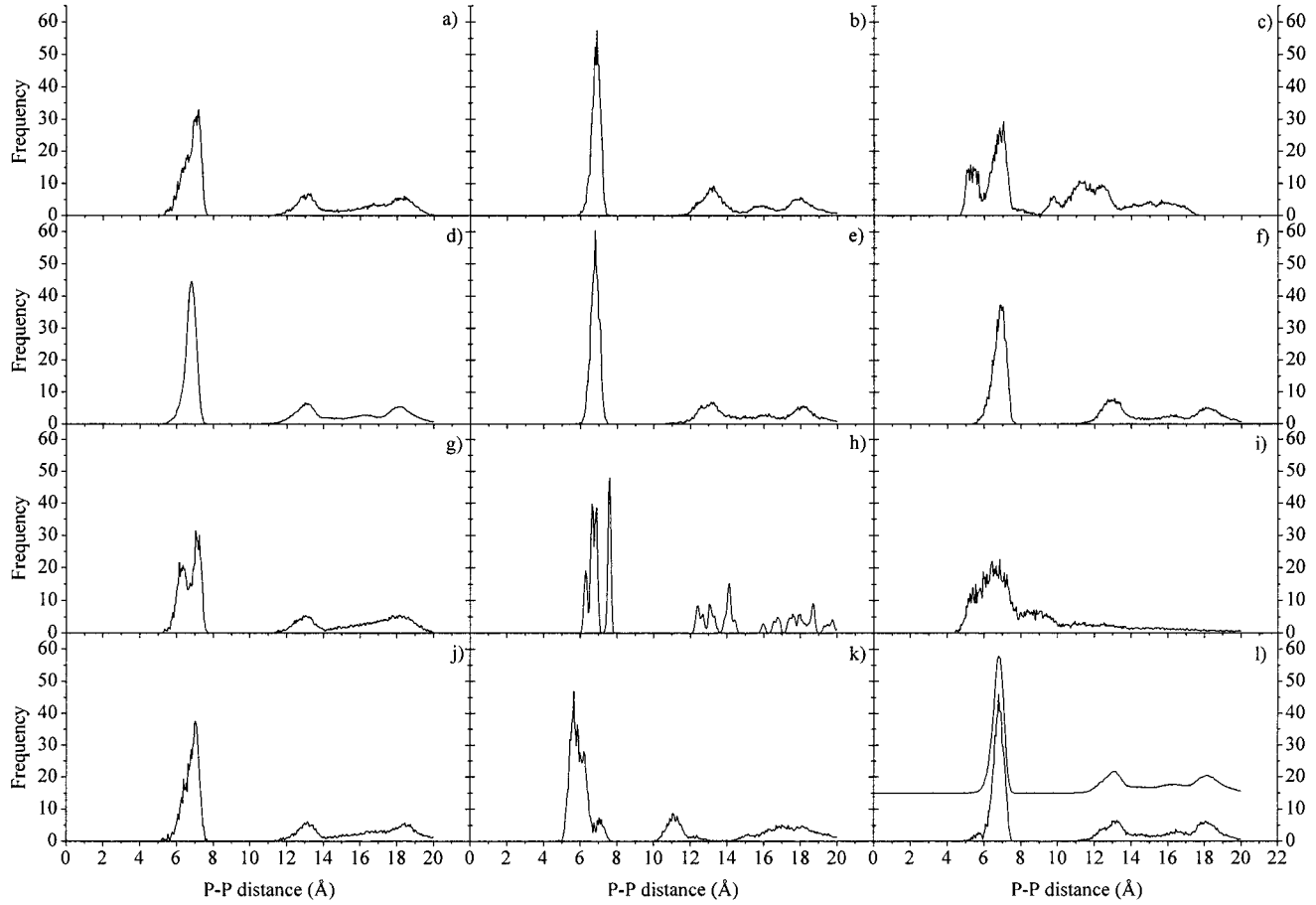

FIGURE 7 Distribution of phosphorus–phosphorus distances of the DNA hexamer from the methods (*a*) AFSH, (*b*) AFSW, (*c*) GSW, (*d*) AFSH (5.03-ns simulation), (*e*) ASH, (*f*) GTR, (*g*) AFSHL, (*h*) ASW, (*i*) GTRS, (*j*) AFSHS, (*k*) GFSW, and (*l*) PME and PME (5.03-ns simulation shifted 15 upward).

PME methods, respectively, from the initial B-DNA structure. The rms fluctuations of the bases were the same for both truncation methods, but the fluctuations of the backbone were slightly larger for the AFSH method. Here it is appropriate to comment on the significance of rms deviations as the criterion for judging the stability of molecular dynamics simulations. A number of simulations carried out in the same manner but with different values of the random seed for the assignment of the velocity distribution, showed that the rms deviations from the starting structure were different (Auffinger et al., 1995; Auffinger and Westhof, 1996). This indicates that differences in the rms deviations of ~0.2 Å are not significant for judging the quality or stability of this kind of system. A study by Feller et al. (1996) showed that the relative rms force error was smaller for the PME method compared to the AFSH method, but still, both algorithms generated accurate and stable trajectories with similar rms deviations as shown here. It should be noted that both version 22 (MacKerell et al., 1995) and version 27 (Foloppe and MacKerell, 2000) of the CHARMM energy function were developed using 12-Å spherical cutoffs and either the ASH or the AFSH method.

TABLE 4 Elapsed time (s) required for simulating 1.0 ps using different truncation methods and 1, 2, 4, or 8 nodes

Cutoff Method	1 Node	2 Nodes	4 Nodes	8 Nodes
ASH	1044	537 (1.94)	301 (3.47)	202 (5.17)
AFSHS	395	207 (1.91)	136 (2.90)	121 (3.28)
AFSH	922	473 (1.95)	271 (3.41)	188 (4.91)
AFSHL	2527	1274 (1.98)	681 (3.71)	398 (6.35)
AFSH-SDB	194	102 (1.90)	67 (2.90)	60 (3.23)
AFSW	1066	547 (1.95)	306 (3.48)	206 (5.18)
ASW	965	495 (1.95)	285 (3.38)	191 (5.05)
PME	1426	763 (1.87)	426 (3.34)	289 (4.94)
GSW	842	444 (1.90)	257 (3.28)	184 (4.57)
GFSW	842	447 (1.88)	260 (3.24)	184 (4.57)
GTRS	270	162 (1.67)	113 (2.39)	109 (2.48)
GTR	659	364 (1.81)	215 (3.06)	161 (4.08)

The time for one processor divided by the time for the parallel processors is shown in parenthesis.

An important factor in molecular simulations is how to most efficiently use the available computational resources. From the present analysis, it is evident that the atom-based force-shift method with a cutoff of 12.0 Å is faster than the

PME method with a direct space nonbonded cutoff of 12.0 Å. By lowering the cutoff radius, the PME method becomes faster and competes in speed with the AFSH method.

The rms deviation from the initial B-DNA structure clearly showed that a B-DNA conformation was obtained using the CHARMM version 27 parameters (Foloppe and MacKerell, 2000). This observation was independent of which truncation method, the AFSH or the PME, was used. Both the bases and the backbone were found in the B-DNA form. Another study previously obtained an A-DNA form of a dodecamer using the CHARMM version 22 parameters (MacKerell et al., 1995) and the Ewald method (Yang and Pettitt, 1996). Other studies have shown that the AMBER parameters give slightly more B-DNA-like structures (Cheatham and Kollman, 1996) or, for several-nanosecond simulations, a slightly A-DNA-like conformation (Feig and Pettitt, 1997). In the present study, different truncation methods were found to yield accurate and stable nanosecond simulations.

The resulting DNA conformations are clearly dependent on the parameters of the energy function, whereas the stability of the simulation is more influenced by certain truncation methods rather than by the choice of periodic or nonperiodic boundary conditions, or the use of a spherical cutoff or an Ewald summation method. In particular, the group-based methods, which are known to perform poorly (for a recent study see Steinbach and Brooks, 1994), especially for charged systems, and the atom-based potential switching method, yielded very unsatisfactory results. Other spherical cutoff truncations performed very well, at least with cutoffs of 12 Å or longer, as did the PME and a nonperiodic simulation using the atom-based force-shift method. The superiority of PME over spherical cutoff methods in general, which, from time to time has been claimed to exist, thus seems to stem from comparing PME with one particular, and inferior, spherical truncation scheme (Cheatham et al., 1995; Norberto de Souza and Ornstein, 1999). The present results were obtained for a fully charged short DNA duplex, where end effects could be expected to be quite important, and we do not expect our conclusions to change for larger DNA molecules.

This work was supported by the Swedish Natural Science Research Foundation, the Magnus Bergvall Foundation, and by the Swedish Research Council for Engineering Sciences. J.N. acknowledges a postdoctoral fellowship from The Swedish Foundation for International Cooperation in Research and Higher Education.

REFERENCES

Allen, M. P., and D. J. Tildesley. 1987. Computer simulation of liquids. Oxford University Press, New York.

Auffinger, P., S. Louise-May, and E. Westhof. 1995. Multiple molecular dynamics simulations of the anticodon loop of $tRNA^{Asp}$ in aqueous solution with counterions. *J. Am. Chem. Soc.* 117:6720–6726.

Auffinger, P., and E. Westhof. 1996. H-bond stability in the $tRNA^{Asp}$ anticodon hairpin: 3 ns of multiple molecular dynamics simulations. *Biophys. J.* 71:940–954.

Auffinger, P., and E. Westhof. 1998. Molecular dynamics: simulations of nucleic acids. *In* Encyclopedia of Computational Chemistry. John Wiley & Sons, New York. 1628–1639.

Arnott, S., P. J. C. Smith, and R. Chandrasekaran. 1976. Atomic coordinates and molecular conformations for DNA–DNA, RNA–RNA, and DNA–RNA helices. *In* CRC Handbook of Biochemistry and Molecular Biology: Nucleic Acids, 3rd ed., Vol. 2. G. D. Fasman, editor. CRC Press, Cleveland, OH. 411–422.

Berendsen, H. J. C. 1993. Electrostatic interactions. *In* Computer Simulations of Biomolecular Systems: Theoretical and Experimental Applications. ESCOM, Leiden, The Netherlands.161–181.

Berendsen, H. J. C., W. F. van Gunsteren, H. R. J. Zwinderman, and R. G. Geurtsen. 1986. Simulations of proteins in water. *Ann. N.Y. Acad. Sci.* 482:269–285.

Berendsen, H. J. C., J. P. M. Postma, W. F. van Gunsteren, A. DiNola, and J. R. Haak. 1984. Molecular dynamics with coupling to an external bath. *J. Comput. Phys.* 81:3684–3690.

Bevan, D. R., L. Li, L. G. Pedersen, and T. A. Darden. 2000. Molecular dynamics simulations of the $d(CCAACGTTGG)_2$ decamer: influence of the crystal environment. *Biophys. J.* 78:668–682.

Borer, P. N., S. R. LaPlante, A. Kumar, N. Zanatta, A. Martin, A. Hakkinen, and G. C. Levy. 1994. ^{13}C-NMR relaxation in three DNA oligonucleotide duplexes: model-free analysis of internal and overall motion. *Biochemistry.* 33:2441–2450.

Brooks, B. R., R. E. Bruccoleri, B. D. Olafson, D. J. States, S. Swaminathan, and M. Karplus. 1983. CHARMM: a program for macromolecular energy, minimization, and dynamics calculations. *J. Comp. Chem.* 4:187–217.

Brooks, C. L., III, B. M. Pettitt, and M. Karplus. 1985. Structural and energetic effects of truncating long ranged interactions in ionic and polar fluids. *J. Chem. Phys.* 83:5897–5908.

Cheatham, T. E., III, and B. R. Brooks. 1999. Recent advances in molecular dynamics simulation towards the realistic representation of biomolecules in solution. *Theor. Chem. Acc.* 99:279–288.

Cheatham, T. E., III, P. Cieplak, and P. A. Kollman. 1999. A modified version of the Cornell et al. force field with improved sugar pucker phases and helical repeat. *J. Biomol. Struct. Dyn.* 16:845–862.

Cheatham, T. E., III, and P. A. Kollman. 1996. Observation of the A-DNA to B-DNA transition during unrestrained molecular dynamics in aqueous solution. *J. Mol. Biol.* 259:434–444.

Cheatham, T. E., III, J. L. Miller, T. Fox, T. A. Darden, and P. A. Kollman. 1995. Molecular dynamics simulations on solvated biomolecular systems: the particle mesh Ewald method leads to stable trajectories of DNA, RNA, and proteins. *J. Am. Chem. Soc.* 117:4193–4194.

Cieplak, P., T. E. Cheatham, III, and P. A. Kollman. 1997. Molecular dynamics simulations find that 3′ phosphoramidate modified DNA duplexes undergo a B to A transition and normal DNA duplexes an A to B transition. *J. Am. Chem. Soc.* 119:6722–6730.

Cornell, W. D., P. Cieplak, C. I. Bayly, I. R. Gould, K. M. Merz, Jr., D. M. Ferguson, D. C. Spellmeyer, T. Fox, J. W. Caldwell, and P. A. Kollman. 1995. A new force field for molecular mechanical simulation of nucleic acids and proteins. *J. Am. Chem. Soc.* 117:5179–5197.

Darden, T., L. Perera, L. Li, and L. Pedersen. 1999. New tricks for modelers from the crystallography toolkit: the particle mesh Ewald algorithm and its use in nucleic acid simulations. *Structure.* 7:R55–R60.

Darden, T., A. Toukmaji, and L. G. Pedersen. 1997. Long-range electrostatic effects in biomolecular simulations. *J. Chim. Phys.* 94:1346–1364.

Darden, T., D. York, and L. Pedersen. 1993. Particle mesh Ewald: an $N\cdot\log(N)$ method for Ewald sums in large systems. *J. Chem. Phys.* 98:10089–10092.

Deserno, M., and C. Holm. 1998. How to mesh up Ewald sums. I. A theoretical and numerical comparison of various particle mesh routines. *J. Chem. Phys.* 109:7678–7693.

Duan, Y., P. Wilkosz, M. Crowley, and J. M. Rosenberg. 1997. Molecular dynamics simulation study of DNA dodecamer d(CGCGAATTCGCG) in solution: conformation and hydration. *J. Mol. Biol.* 272:553–572.

Duan, Y., P. Wilkosz, and J. M. Rosenberg. 1996. Dynamic contributions to the DNA binding entropy of the *Eco*RI and *Eco*RV restriction endonucleases. *J. Mol. Biol.* 264:546–555.

Essmann, U., L. Perera, M. L. Berkowitz, T. Darden, H. Lee, and L. G. Pedersen. 1995. A smooth particle mesh Ewald method. *J. Chem. Phys.* 103:8577–8593.

Ewald, P. P. 1921. Die berechnung optischer und elektrostatischer Gitterpotentiale. *Ann. Phys.* 64:253–287.

Feig, M., and B. M. Pettitt. 1997. Experiment vs force fields: DNA conformation from molecular dynamics simulations. *J. Phys. Chem. B.* 101:7361–7363.

Feig, M., and B. M. Pettitt. 1998. Structural equilibrium of DNA represented with different force fields. *Biophys. J.* 75:134–149.

Feig, M., and B. M. Pettitt. 1999. Sodium and chlorine ions as part of the DNA solvation shell. *Biophys. J.* 77:1769–1781.

Feller, S. E., R. W. Pastor, A. Rojnuckarin, S. Bogusz, and B. R. Brooks. 1996. Effect of electrostatic force truncation on interfacial and transport properties of water. *J. Phys. Chem.* 100:17011–17020.

Foloppe, N., and A. D. MacKerell, Jr. 2000. All-atom empirical force field for nucleic acids. 1. Parameter optimization based on small molecule and condensed phase macromolecular target data. *J. Comp. Chem.* 21: 86–104.

Guenot, J., and P. A. Kollman. 1992. Molecular dynamics studies of a DNA-binding protein. 2. An evaluation of implicit and explicit solvent models for the molecular dynamics simulation of the *Escherichia coli trp* repressor. *Prot. Sci.* 1:1185–1205.

Guenot, J., and P. A. Kollman. 1993. Conformational and energetic effects of truncating nonbonded interactions in an aqueous protein dynamics simulation. *J. Comp. Chem.* 14:295–311.

Harvey, S. C. 1989. Treatment of electrostatic effects in macromolecular modeling. *Proteins.* 5:78–92.

Hermans, J. 1997. Insight via simulations: publishing results and methods. *Proteins.* 2:27:i.

Jorgensen, W. L., J. Chandrasekhar, J. D. Madura, R. W. Impey, and M. L. Klein. 1983. Comparison of simple potential functions for simulating liquid water. *J. Chem. Phys.* 79:926–935.

Kitson, D. H., F. Avbelj, J. Moult, D. T. Nguyen, J. E. Mertz, D. Hadzi, and A. T. Hagler. 1993. On achieving better than 1-Å accuracy in a simulation of a large protein: *streptomyces griseus* protease A. *Proc. Natl. Acad. Sci. USA.* 90:8920–8924.

Komeiji, Y., and M. Uebayasi. 1999. Molecular dynamics simulation of the *Hin*-recombinase-DNA complex. *Mol. Simulation*. 21:303–324.

Langley, D. R. 1998. Molecular dynamics simulations of environment and sequence dependent DNA conformations: the development of the BMS nucleic acid force field and comparison with experimental results. *J. Biomol. Struct. Dyn.* 16:487–509.

Lee, H., T. Darden, and L. Pedersen. 1995. Accurate crystal molecular dynamics simulations using particle-mesh-Ewald: RNA dinucleotides - ApU and GpC. *Chem. Phys. Lett.* 243:229–235.

Loncharich, R. J., and B. R. Brooks. 1989. The effects of truncating long-range forces on protein dynamics. *Proteins.* 6:32–45.

MacKerell, A. D., Jr. 1997. Influence of magnesium ions on duplex DNA structural, dynamic, and solvation properties. *J. Phys. Chem. B.* 101: 646–650.

MacKerell, A. D., Jr., J. Wiórkiewics-Kuczera, and M. Karplus. 1995. An all-atom empirical energy function for the simulation of nucleic acids. *J. Am. Chem. Soc.* 117:11946–11975.

McCammon, J. A., and S. C. Harvey. 1987. Dynamics of Proteins and Nucleic Acids. Cambridge University Press, Cambridge, U.K.

Miaskiewics, K., J. Miller, M. Cooney, and R. Osman. 1996. Computational simulations of DNA distortions by a *cis*,*syn*-cyclobutane thymine dimer lesion. *J. Am. Chem. Soc.* 118:9156–9163.

Norberg, J. 1995. A biophysical perspective of dynamics, structure, and thermodynamics of nucleic acids. Molecular dynamics simulations of nucleic acids. Ph.D. thesis, Karolinska Institutet, Stockholm, Sweden.

Norberg, J., and L. Nilsson. 1994. High-pressure molecular dynamics of a nucleic acid fragment. *Chem. Phys. Lett*. 224:219–224.

Norberg, J., and L. Nilsson. 1995. NMR relaxation times, dynamics, and hydration of a nucleic acid fragment from molecular dynamics simulations. *J. Phys. Chem.* 99:14876–14884.

Norberg, J., and L. Nilsson. 1996a. Constant pressure molecular dynamics simulations of the dodecamers: $d(GCGCGCGCGCGC)_2$ and $r(GCGCGCGCGCGC)_2$. *J. Chem. Phys.* 104:6052–6057.

Norberg, J., and L. Nilsson. 1996b. Internal mobility of the oligonucleotide duplexes $d(TCGCG)_2$ and $d(CGCGCG)_2$ in aqueous solution from molecular dynamics simulations. *J. Biomol. NMR.* 7:305–314.

Norberg, J., and L. Nilsson. 1996c. Potential of mean force calculations of the stacking–unstacking process in single-stranded deoxyribodinucleoside monophosphates. *Biophys. J.* 69:2277–2285.

Norberg, J., and L. Nilsson. 1998. Solvent influence on base stacking. *Biophys. J.* 74:394–402.

Norberto de Souza, O., and R. L. Ornstein. 1997a. Effects of periodic box size on aqueous molecular dynamics simulation of a DNA dodecamer with particle-mesh Ewald method. *Biophys. J.* 72:2395–2397.

Norberto de Souza, O., and R. L. Ornstein. 1997b. Effects of warmup protocol and sampling time on convergence of molecular dynamics simulations of a DNA dodecamer using AMBER 4.1 and particle-mesh Ewald method. *J. Biomol. Struct. Dyn.* 14:607–611.

Norberto de Souza, O., and R. L. Ornstein. 1999. Molecular dynamics simulations of a protein–protein dimer: particle-mesh Ewald electrostatic model yields far superior results to standard cutoff model. *J. Biomol. Struct. Dyn.* 16:1205–1218.

Pastor, N., L. Pado, and H. Weinstein. 1997. Does TATA matter? A structural exploration of the selectivity determinants in its complexes with TATA box-binding protein. *Biophys. J.* 73:640–652.

Pollock, E. L., and J. Glosli. 1996. Comments on P^3M, FMM, and the Ewald method for large periodic Coulombic systems. *Comp. Phys. Comm.* 95:93–110.

Prevost, M., D. van Belle, G. Lippens, and S. Wodak. 1990. Computer simulations of liquid water: treatment of long-range interactions. *Mol. Phys.* 71:587–603.

Ryckaert, J.-P., G. Ciccotti, and H. J. C. Berendsen. 1977. Numerical integration of the Cartesian equations of motion of a system with constraints: molecular dynamics of n-alkanes. *J. Comp. Phys.* 23: 327–341.

Saenger, W. 1988. Principles of Nucleic Acid Structure. Springer-Verlag, New York.

Sagui, C., and T. A. Darden. 1999. Molecular dynamics simulations of biomolecules: long-range electrostatic effects. *Annu. Rev. Biophys. Biomol. Struct.* 28:155–179.

Saito, M. 1992. Molecular dynamics simulations of proteins in water without the truncation of long-range Coulomb interactions. *Mol. Simul.* 8:321–333.

Saito, M. 1994. Molecular dynamics simulations of proteins in solution: artifacts caused by the cutoff approximation. *J. Chem. Phys.* 101: 4055–4061.

Schreiber, H., and O. Steinhauser. 1992a. Cutoff size does strongly influence molecular dynamics results on solvated polypeptides. *Biochemistry.* 31:5856–5860.

Schreiber, H., and O. Steinhauser. 1992b. Molecular dynamics studies of solvated polypeptides: why the cut-off scheme does not work. *Chem. Phys.* 168:75–89.

Schreiber, H., and O. Steinhauser. 1992c. Taming cut-off induced artifacts in molecular dynamics studies of solvated polypeptides. The reaction field method. *J. Mol. Biol.* 228:909–923.

Shields, G. C., C. A. Laughton, and M. Orozco. 1997. Molecular dynamics simulations of the d(T·A·T) triple helix. *J. Am. Chem. Soc.* 119: 7463–7469.

Smith, P. E., and B. M. Pettitt. 1991. Peptides in ionic solutions: a comparison of the Ewald and switching function techniques. *J. Chem. Phys.* 95:8430–8440.

Smith, P. E., and B. M. Pettitt. 1995. Efficient Ewald electrostatic calculations for large systems. *Comp. Phys. Commun.* 91:339–344.

Smith, P. E., and B. M. Pettitt. 1996. Ewald artifacts in liquid state molecular dynamics simulations. *J. Chem. Phys.* 105:4289–4293.

Smith, P. E., and W. F. van Gunsteren. 1993. Methods for the evaluation of long range electrostatic forces in computer simulations of molecular systems. *In* Computer Simulations of Biomolecular Systems: Theoretical and Experimental Applications. ESCOM, Leiden, The Netherlands.182–212.

Steinbach, P. J., and B. R. Brooks. 1994. New spherical-cutoff methods for long-range forces in macromolecular simulation. *J. Comp. Chem.* 15: 667–683.

van Gunsteren, W. F., and H. J. C. Berendsen. 1990. Computer simulation of molecular dynamics: methodology, applications, and perspectives in chemistry. *Angew. Chem. Int. Ed. Engl.* 29:992–1023.

Weber, W., P. H. Hünenberger, and J. A. McCammon. 2000. Molecular dynamics simulations of a polyalanine octapeptide under Ewald boundary conditions: influence of artificial periodicity on peptide conformation. *J. Phys. Chem. B.* 104:3668–3675.

Weerasinghe, S., P. E. Smith, V. Mohan, Y.-K. Cheng, and B. M. Pettitt. 1995. Nanosecond dynamics and structure of a model DNA triple helix in saltwater solution. *J. Am. Chem. Soc.* 117:2147–2158.

Yang, L., and B. M. Pettitt. 1996. B to A transition of DNA on the nanoseond time scale. *J. Phys. Chem.* 100:2564–2566.

York, D. M., T. A. Darden, and L. G. Pedersen. 1993. The effect of long-range electrostatic interactions in simulations of macromolecular crystals: a comparison of the Ewald and truncated list methods. *J. Chem. Phys.* 99:8345–8348.

York, D. M., W. Yang, H. Lee, T. Darden, and L. G. Pedersen. 1995. Toward the accurate modeling of DNA: the importance of long-range electrostatics. *J. Am. Chem. Soc.* 117:5001–5002.

Young, M. A., G. Ravishanker, and D. L. Beveridge. 1997. A 5-nanosecond molecular dynamics trajectory for B-DNA: analysis of structure, motion, and solvation. *Biophys. J.* 73:2313–2336.

Zuegg, J., and J. E. Gready. 1999. Molecular dynamics simulations of human prion protein: importance of correct treatment of electrostatic interactions. *Biochemistry.* 38:13862–13876.